Submicron-Resolution Study of a Thin Ni Crystal Using a Brightness-Enhanced Positron Reemission Microscope

G. R. Brandes,[1] K. F. Canter,[1] and A. P. Mills, Jr.[2]
[1]*Physics Department, Brandeis University, Waltham, Massachusetts 02254*
[2]*AT&T Bell Laboratories, Murray Hill, New Jersey 07974*
(Received 13 June 1988)

A 1500-Å Ni(100) film is back illuminated with 5-keV positrons from a brightness-enhanced slow positron beam. Some of the positrons diffuse through the film and are emitted from the front surface by virtue of the Ni having a negative positron affinity. An immersion objective and projector lens form a 1150× image of the reemitted positrons at a 2D position-sensitive detector. With a resolution of 3000 ± 1000 Å we observe patches attributable to positron trapping at boundary layers inside the film. The advantages and ultimate capabilities of the positron reemission microscope are also discussed.

PACS numbers: 07.80.+x, 68.55.Ln, 78.70.Bj

There are numerous ways to form images of small objects by the scattering, emission, and tunneling of various particles and waves, or by near contact with a material probe. There are many ways to improve visibilities by staining, replication, diffraction, and single-particle detection. Although the electron microscope in its many forms has evolved to being capable of atomic resolution,[1] it is important to continue to investigate alternate methods of imaging that might offer qualitatively different sensitivity, contrast, and resolution. The first microscope to use positrons[2] was the equivalent of the transmission electron microscope. The positron reemission microscope as proposed by Hulett, Dale, and Pendyala[3] operates on a principle fundamentally different from those employed in existing microscopes. We would like to report here the operation of a positron reemission microscope (PRM) having a resolution comparable to that of conventional light microscopy, and with which we have observed interesting features on a micron scale. We are encouraged to project that it will be possible to obtain resolutions of a few angstroms and to image single vacancies in a crystal or unstained molecules of biological interest.

We have recently demonstrated the principle of the PRM by imaging positrons spontaneously emitted after being implanted into a material having a negative positron affinity.[4] Positrons are implanted at kiloelectronvolt energies into one side of a thin foil, diffuse to the other side, and are emitted with a kinetic energy roughly given by the negative of the positron work function ϕ_+.[5] Contrast in the positron image can be provided by nonuniform film thickness, variable bulk defect density, patches of different crystal orientations, contaminant layers that affect ϕ_+ and hence the emission probability, and adsorbed molecules or larger structures that attenuate the emitted positrons. In our first experiment we imaged at 330× the shadow of a mesh overlaying an apparently featureless polycrystalline Ni foil using a single immersion objective lens.[4] We have now increased the magnification to 1150× by the addition of a projector lens and are able to image features of the film itself, with a resolution of 3000 ± 1000 Å.

The basis for any practical positron microscope is a bright source of low-energy positrons. The technique of obtaining slow positrons of a few electronvolts from a solid surface irradiated by β decay or pair production positrons is well known.[5] Slow positrons may be accelerated, formed into a beam and brought to a sharp focus to illuminate a portion of a surface with a flux density, J, limited in magnitude by the brightness of the positron source. Of several contributions to the resolution of a positron microscope there is a counting-statistics-limited term proportional to $J^{-1/2}$ which is important to minimize. By repeated stages of acceleration, focusing, and remoderation, we may enhance the brightness and hence J with only a small decrease in the total intensity.[6] While one might be able to obtain a comparable flux density by using a higher-flux positron beam, a few orders of magnitude of the flux would be wasted if one did not employ brightness enhancement.

The positron beam[7] for our experiment employs two stages of reflection-mode brightness enhancement.[8] An 80-mCi Co-58 source and 9-mm-diam W(110) moderator produces the primary slow positron flux of 1.8×10^5 s^{-1}. The beam is reduced to 1 mm diameter on the first W(110) remoderator and is reemitted from a 100-μm spot on the second W(110) remoderator with a flux of 10^4 s^{-1}. The positrons are accelerated to 5 keV by a 1.5-mm-diam tube lens[9] and brought to 20-μm-diam focus on the back of the sample. Positrons emitted from the front of the Ni crystal are magnified by a three-element immersion objective lens (cathode lens),[4,10] magnified further by a projector lens (einzel lens) and projected onto a channel electron multiplier array coupled to a positron-sensitive 2D resistive anode readout.

The sample foil was a free-standing 1500-Å-thick Ni(100) crystal grown by evaporation onto a NaCl crystal.[11] The film was floated off the substrate and back

supported on a hexagonal mesh measured to have 108-μm openings (diameter of an inscribed circle) and 20-μm bar widths. The Ni crystal was annealed in vacuum prior to installation in the microscope. A preliminary PRM image of the foil taken with the microbeam defocused and without the projector lens installed is shown in Fig. 1. The magnification measured at the detector plane is 330×, and the exposure time was 8 h. The picture displays a large area of patches of varying positron emission, bordered at the right and lower right by the shadows of three segments of the hexagonal support mesh. The scale is set by the 62-μm distance between the inside corners of the mesh openings. The white 35×35-μm^2 square outline contains a detail (shown at a more sensitive display scale in the inset) that we subsequently examined at higher magnification.

After the data for Fig. 1 were taken, the sample was exposed to air while the projector lens was installed. The sample and ultrahigh vacuum chamber were subsequently baked at 105 °C for 24 h to reduce the background pressure to below 10^{-10} Torr. Figure 2(a) is a PRM image of the portion of the Ni film that we identify with the white box in Fig. 1. The image is inverted by the projector lens and part of a support mesh bar is shown at the lower left. From the length of the central gray bar we find that the projector magnification is 11.5× (the objective forms a 100× image at the projector focal plane) and the total magnification is 1150×. Figure 2(b) shows the same portion of the film after it was heated *in situ* by electron bombardment for 5 min and cooled slowly to room temperature. A very bright patch appears in the upper left quadrant and the positron emissivity of the long bar has increased and its length diminished.

Because of the manner of preparation of the sample, variations in the Ni film thickness are probably not responsible for the contrast evident in Figs. 1 and 2. Dislocations,[12] which are present even in well annealed materials (typically $\approx 10^7$ cm^{-2}), may be introduced at high density when the crystal is grown or when strain is applied. When a strained specimen is annealed at moderate temperature, dislocations tend to become ordered, resulting in low angle or tilt boundaries. We thus find it reasonable to assume that the different patches of emissivity are due to the trapping of positrons at

FIG. 1. A low magnification (330×) PRM image of a Ni(100) film obtained over an 8-h exposure with an immersion objective lens. The white box indicates a portion of the film that was imaged at higher magnification (see Fig. 2) with the addition of a projector lens. This region is also shown in a higher contrast mode in the upper left inset. The whitest areas correspond to an average of 30 counts/pixel (256×256 pixels for the entire frame), with the exception of the detector hot spot on the center left area of the detector. The dark noise for all images is 0.1 counts/pixel h.

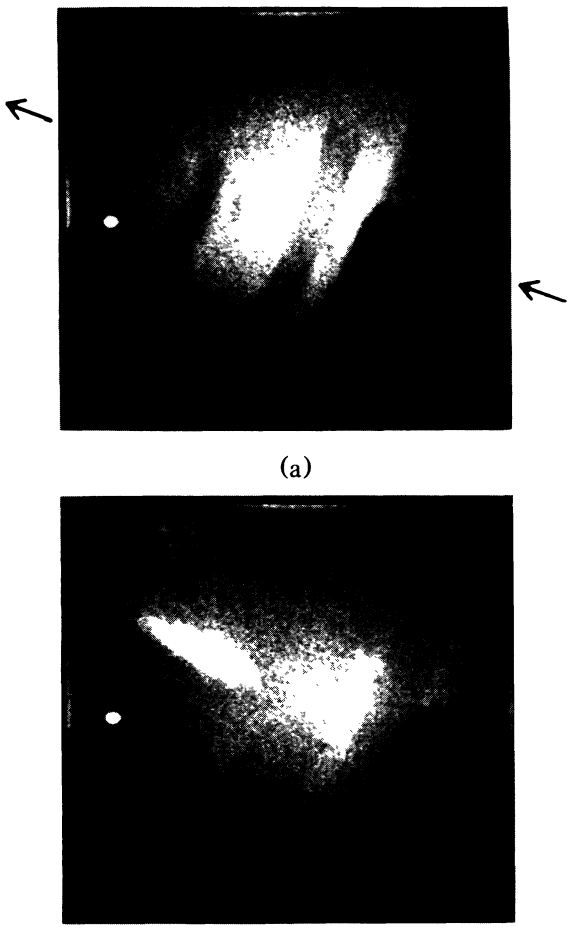

(a)

(b)

FIG. 2. (a) 1150× PRM image of the region of interest outlined in Fig. 1. Arrows indicate the path of integration used (see Fig. 3) to determine the sharpness of the edges of some of the features. (b) The same region following 5 min of electron bombardment from behind. In both cases, the images were obtained over a 14-h period with the whitest areas representing 40 counts/pixel in (a) and 65 counts/pixel in (b).

different rates by various boundaries parallel to the surface of the material. We expect larger tilt angles to result in more trapping and hence correspond to darker areas on the PRM image. The bright regions formed after we anneal the sample are further evidence of the strain relief and recrystallization processes. Surface contamination could also contribute to some of the observed emission variations.

To obtain an estimate of our resolution, we examine in Fig. 3 a cut through the data of Fig. 2(a) on a line cutting at a right angle through the sharpest feature. The line is indicated by the arrows in Fig. 2(a), and we have integrated over a strip 5 pixels wide. Taking into account the one-pixel effective detector resolution, we estimate that the sudden rises at integration-step numbers 89 and 103 correspond to a PRM resolution of 3000 ± 1000 Å full width at half maximum.

The ultimate resolution $2\Delta r$ of the PRM depends on the incident flux density, J, the de Broglie wavelength λ of the reemitted positrons, and the transverse (E_T) and normal ($E_\perp$) components of the positron emission energy[4]:

$$(2\Delta r)^2 = 40\alpha/\epsilon K^2 Jt + \beta\lambda^2 + E_T[(E_\perp^{\max})^{1/2} - (E_\perp^{\min})^{1/2}]^2/U^2. \quad (1)$$

Here K is the contrast of the image, ϵ is the average positron reemission probability, t is the exposure time, and U is the electric field in front of the sample; α and β are dimensionless constants of order 1. If the emitting foil is locally regarded as a good single crystal, then we can assume[13] $E_T = kT$, $E_\perp^{\min} = -\phi_+$, and $E_\perp^{\max} = -\phi_+ + kT$, where T is the sample temperature, provided the positrons have thermalized. The third term in Eq. (1) then becomes $(kT)^3/U^2(-\phi_+)$ and at 77 K equals $(3.6\ \text{Å})^2$ with $-\phi_+ = 1$ eV and $U = 10^4$ V/cm. The second term, $\approx\beta(10\ \text{Å})^2$, will be dominant if $Jt > 10^{17}\ e^+/\text{cm}^2$, if we assume $\epsilon \approx 0.1$ and $K \approx 0.5$. With our present beam, $Jt \approx 10^{14}\ e^+/\text{cm}^2$ for a 12-h integration. The addition of a 100-mCi Na-22 source, a solid Ne positron moderator,[14] and cooled remoderators would give the 3-orders-of-magnitude flux increase needed to exceed the positron wavelength limit.

The $\approx$ 10-Å de Broglie wavelength of positrons emitted from Ni imposes a limit on the PRM resolution and also raises the possibility of an interesting contrast mechanism when molecular structures are imaged on the surface of the emitting foil. The emission of a positron from the Ni is determined in part by the potential-barrier reflection encountered by the positron as it escapes into the vacuum.[15] If, however, a molecule is added on top of the foil, additional interference effects between the scattering of the positron from the Ni-vacuum potential barrier and the atoms of the molecule could strongly affect the local emission rate $\epsilon(x,y)$. Thus for sufficiently thin overlaying structures, $\epsilon(x,y)$ would exhibit features attributable to the three-dimensional nature of the structure, rather than just its two-dimensional projection. In two dimensions parallel to the foil, structural information on a scale less than the 10-Å positron de Broglie wavelength can be possible if the transverse coherence length exceeds the size of the object be-

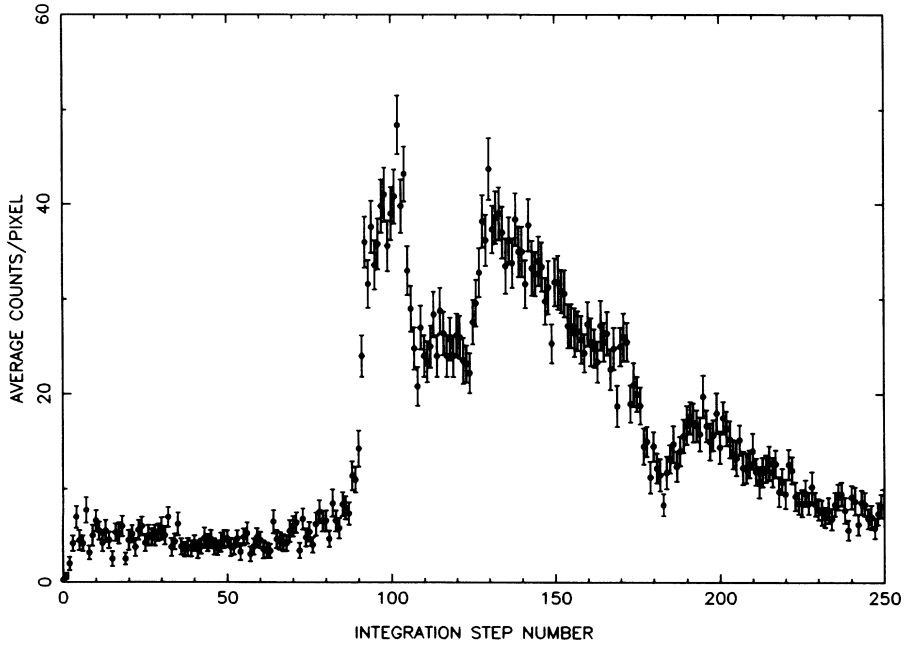

FIG. 3. Average counts/pixel determined from a 0.14×0.68-μm^2 region rastered along the path indicated by the arrows in Fig. 2(a). One step equals one pixel equals 1300 Å.

ing imaged. In this case we could envision a form of positron holography analogous to in-line electron holography.[16]

In summary we have constructed a brightness-enhanced positron reemission microscope, demonstrated its 3000-Å resolution, and with 1150× magnification observed features in a thin Ni foil that can be explained by positron trapping at low angle or tilt boundaries. We anticipate that we should soon attain a resolution of a few tens of angstroms, at which point small defect structures and large adsorbed molecules might be examined in detail.

The collaboration of T. N. Horsky and P. H. Lippel on the earlier phases of this work is gratefully acknowledged. We would also like to thank Professor S. Berko and Professor E. Jensen for numerous helpful discussions. This work is supported in part by National Science Foundation Grant No. DMR 8519524 and National Institutes of Health Grant No. BRSGS07RR-07044.

[1]E. Ruska, Rev. Mod. Phys. **59**, 627 (1987); A. V. Crewe, Science **221**, 325 (1983); G. Binnig and H. Rohrer, IBM J. Res. Dev. **30**, 355 (1986).

[2]J. Van House and A. Rich, Phys. Rev. Lett. **60**, 169 (1988).

[3]L. D. Hulett, J. M. Dale, and S. Pendyala, Mater. Sci. Forum **2**, 133 (1984). We note that the direct electron analog of the PRM could be obtained with a negative affinity electron emitting sample. See, for example, H. J. Drouhin, C. Hermann, and G. Lampel, Phys. Rev. B **31**, 3859 (1985).

[4]G. R. Brandes, K. F. Canter, T. N. Horsky, and A. P. Mills, Jr., Appl. Phys. **46**, 335 (1988).

[5]For an up-to-date review of positron interactions near a surface, see K. G. Lynn and P. J. Schultz, Rev. Mod. Phys. **60**, 701 (1988).

[6]A. P. Mills, Jr., Appl. Phys. **23**, 189 (1980).

[7]K. F. Canter, G. R. Brandes, T. N. Horsky, P. H. Lippel, and A. P. Mills, Jr., in *Atomic Physics with Positrons,* edited by J. W. Humbertson and E. A. G. Armour (Plenum, London, 1987), 1st. ed., and references therein.

[8]K. F. Canter, in *Positron Scattering Gases,* edited by J. W. Humbertson and M. R. C. McDowell (Plenum, New York, 1984), p. 219; W. E. Frieze, D. W. Gidley, and K. G. Lynn, Phys. Rev. B **31**, 5628 (1985).

[9]G. R. Brandes, K. F. Canter, T. N. Horsky, P. H. Lippel, A. P. Mills, Jr., Rev. Sci. Instrum. **59**, 228 (1988).

[10]E. Brüche and H. Johannson, Naturwiss. **20**, 353 (1932).

[11]Samples obtained from J. Chevallier, University of Aarhus, Denmark.

[12]J. Corish, in *Defects in Solids,* edited by A. V. Chadwick and M. Terenz (Plenum, London, 1985), pp. 1–50.

[13]C. A. Murray and A. P. Mills, Jr., Solid State Commun. **34**, 789 (1980); D. A. Fischer, K. G. Lynn, and D. W. Gidley, Phys. Rev. B **33**, 4479 (1986).

[14]A. P. Mills, Jr. and E. M. Gullikson, Appl. Phys. Lett. **49**, 1121 (1986).

[15]R. M. Nieminen and J. Oliva, Phys. Rev. B **22**, 2226 (1980).

[16]A. Tonomura, Rev. Mod. Phys. **59**, 639 (1987).

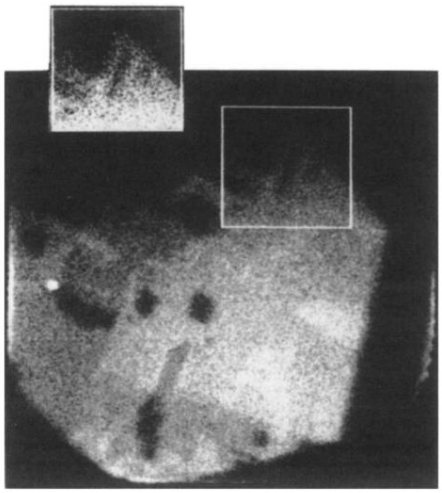

FIG. 1. A low magnification (330×) PRM image of a Ni(100) film obtained over an 8-h exposure with an immersion objective lens. The white box indicates a portion of the film that was imaged at higher magnification (see Fig. 2) with the addition of a projector lens. This region is also shown in a higher contrast mode in the upper left inset. The whitest areas correspond to an average of 30 counts/pixel (256×256 pixels for the entire frame), with the exception of the detector hot spot on the center left area of the detector. The dark noise for all images is 0.1 counts/pixel h.

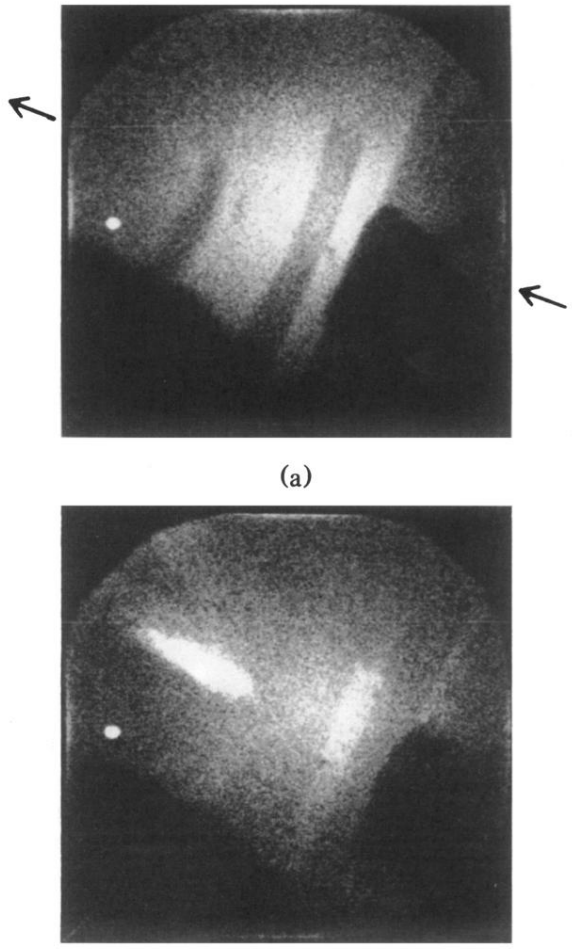

(a)

(b)

FIG. 2. (a) 1150× PRM image of the region of interest outlined in Fig. 1. Arrows indicate the path of integration used (see Fig. 3) to determine the sharpness of the edges of some of the features. (b) The same region following 5 min of electron bombardment from behind. In both cases, the images were obtained over a 14-h period with the whitest areas representing 40 counts/pixel in (a) and 65 counts/pixel in (b).